A R C H I V E O F M E C H A N I C A L E N G I N E E R I N G

VOL. LXII 2015 Number 2

10.1515/meceng-2015-0011

Key words: Navier solution, simply supported plate, two-variable refined plate theory, Winkler elastic foundation

JAFAR ROUZEGAR [*], *REZA ABDOLI SHARIFPOOR* [**]

FLEXURE OF THICK PLATES RESTING ON ELASTIC FOUNDATION USING TWO-VARIABLE REFINED PLATE THEORY

The two-variable refined plate theory is used in this paper for the analysis of thick plates resting on elastic foundation. This theory contains only two unknown parameters and predicts parabolic variation of transverse shear stresses. It satisfies the zero traction on the plate surfaces without using shear correction factor. Using the principle of minimum potential energy, the governing equations for simply supported rectangular plates resting on Winkler elastic foundation are obtained. The Navier method is adopted for solution of obtained coupled governing equations, and several benchmark problems under various loading conditions are solved by present theory. The comparison of obtained results with other common theories shows the excellent efficiency of this theory in modeling thick plates resting on elastic foundation. Also, the effect of foundation modulus, plate thickness and type of loading are studied and the results show that the deflections are decreased by increasing the foundation modulus and plate thickness.

1. Introduction

The most common approaches which are used in plate bending analysis are: the classical thin plate theory (CPT) [1], the first-order shear deformation theory (FSDT) [2, 3], the higher-order shear deformation theory (HSDT) [4, 5] and three-dimensional elasticity theory [6]. The CPT is the simplest theory of plate that gives good results for thin plates but cannot predict the transverse shear stresses along the thickness. The FSDT predicts the constant transverse shear stress along the plate thickness which is not consistent with zero stress conditions on free surfaces. In this theory, the shear correction factor is needed to modify the value of maximum shear stress with that of exact

[*] *Department of Mechanical and Aerospace Engineering, Shiraz University of Technology, Shiraz, 71555-313, Iran; E-mail: rouzegar@sutech.ac.ir*

[**] *Department of Mechanical and Aerospace Engineering, Shiraz University of Technology, Shiraz, 71555-313, Iran; Postgraduate Student.*

value. To avoid the use of shear correction factor and resolve the problem of free surfaces, the higher-order shear deformation theories (HSDTs) were developed. Second-order shear deformation theory of Whitney and Sun [7], third-order shear order shear deformation theory of Hanna and Leissa [8], Reddy [2], Reddy and Phan [3], Bhimaraddi and Stevens [9], Kant [10] and Lo et al. [11] are the most famous HSDTs.

A very recently developed approach is the two-variable refined plate theory (RPT) that contains only two unknown parameters, satisfies the zero stress conditions on free surfaces and does not need the shear correction factor in formulation. This theory was introduced by Shimpi [12] for isotropic plates and then extended to bending and vibration analyses of orthotropic plates [13, 14]. Kim et al. [15, 16] performed buckling analysis of isotropic plates and also bending analysis of laminated composite plates. In the papers by Thai and Kim [17, 18, 19] the problems of free vibrations and buckling for orthotropic and laminate plates were treated. Buckling analysis of nanoplates with nonlocal effect was carried out by Narendar [20] and free vibration analysis of nanoplates considering surface and nonlocal effects was performed by Malekzadeh and Shojaee [21].

Many problems of considerable practical importance can be related to the solution of plates resting on an elastic foundation. Reinforced concrete pavements of highways and airport runways, foundation slabs of buildings, etc., are well-known direct application [22]. Voyiadjis and Kattan [23] carried out the analysis of thick plates on elastic foundation using refined plate theory. Liew et al. [24] studied the moderately thick Mindlin plates on elastic foundation using differential quadrature method. Vibration analysis of a functionally graded rectangular plate on two parameter elastic foundation was presented by Hasani et al. [25]. A parametric study for thick plates resting on elastic foundation with variable soil depth was performed by Korhan et al. [26].

In this paper, the two-variable refined plate theory (RPT) is used for the analysis of thick isotropic plates resting on elastic foundation. To illustrate the accuracy of this theory, several benchmark problems subjected to different loadings are studied. Results obtained by the Navier solution are compared with the results of CPT [1], FSDT [2], HSDT [4], trigonometric shear deformation theory [27] and exact solution of three-dimensional elasticity [6]. Also, the effects of foundation modulus, plate thickness and type of loading on obtained results are studied.

2. Theory and Formulation

Consider a simply supported rectangular plate of length a, width b and thickness h, resting on Winkler elastic foundation. The plate is loaded on its upper surface by a distributed load of intensity $q(x,y)$ acting on z direction. As shown in Fig. 1, the right-handed Cartesian coordinate is located at corner of the middle plane of plate. Accordingly, the plate dimensions ranges are: $0 \le x \le a$, $0 \le y \le b$, $-h/2 \le z \le h/2$.

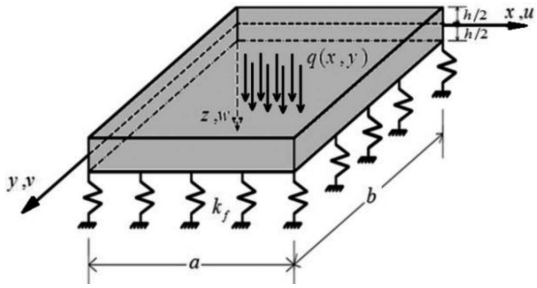

Fig. 1. Geometry and loading of simply supported rectangular plate resting on elastic foundation

2.1. Assumption of Two-variable refined plate theory

The in-plane displacements (u in x-direction, v in y-direction and w in z-direction, as seen in Fig. 1) are negligible relative to the plate thickness. So the strain-displacement relations can be expressed as below:

$$\begin{cases} \varepsilon_x = \dfrac{\partial u}{\partial x}, & \varepsilon_y = \dfrac{\partial v}{\partial y}, & \varepsilon_z = \dfrac{\partial w}{\partial z}, \\ \gamma_{xy} = \dfrac{\partial v}{\partial x} + \dfrac{\partial u}{\partial y}, & \gamma_{yz} = \dfrac{\partial w}{\partial y} + \dfrac{\partial v}{\partial z}, & \gamma_{zx} = \dfrac{\partial w}{\partial x} + \dfrac{\partial u}{\partial z} \end{cases} \tag{1}$$

The transverse displacement w has two components: w_b and w_s, the bending and shear components respectively:

$$w(x,y,t) = w_b(x,y,t) + w_s(x,y,t) \tag{2}$$

The stress normal to the middle plane, σ_z, is small compared with the other stress components and may be neglected in the stress-strain relations. Also, the material of the plate is linear elastic, homogeneous and isotropic. Consequently, the stress-strain relations are:

$$\begin{cases} \sigma_x = \dfrac{E}{(1-\mu^2)}\left(\varepsilon_x + \mu\varepsilon_y\right), & \sigma_y = \dfrac{E}{(1-\mu^2)}\left(\varepsilon_y + \mu\varepsilon_x\right), & \sigma_z = 0, \\ \tau_{xy} = G\gamma_{xy}, & \tau_{yz} = G\gamma_{yz}, & \tau_{zx} = G\gamma_{zx} \end{cases} \tag{3}$$

where E, μ and G are the modulus of elasticity, Poisson's ratio, and the shear modulus, respectively.

The displacements in x and y directions consist of bending and shear components:

$$u = u_b + u_s, \quad v = v_b + v_s \tag{4}$$

The bending components of displacement play the same roles as u and v in classical plate theory. So we can write:

$$u_b = -z\frac{\partial w_b}{\partial x}, \quad v_b = -z\frac{\partial w_b}{\partial y} \tag{5}$$

It may be noted that the bending components of displacement, u_b, v_b and w_b, do not contribute to shear stresses τ_{zx} and τ_{yz}.

2.2. Displacements, moments and shear forces

Based on the assumptions made in the previous section, the displacements can be calculated as [12]:

$$u(x, y, z) = -z\frac{\partial w_b}{\partial x} - f(z)\frac{\partial w_s}{\partial x} \tag{6}$$

$$v(x, y, z) = -z\frac{\partial w_b}{\partial y} - f(z)\frac{\partial w_s}{\partial y} \tag{7}$$

where

$$f(z) = -\frac{1}{4}z + \frac{5}{3}z\left(\frac{z}{h}\right)^2 \tag{8}$$

Equations (6) and (7) are substituted in Eq. (1) to get strains:

$$\varepsilon_x = -z\frac{\partial^2 w_b}{\partial x^2} - f(z)\frac{\partial^2 w_s}{\partial x^2} \tag{9}$$

$$\varepsilon_y = -z\frac{\partial^2 w_b}{\partial y^2} - f(z)\frac{\partial^2 w_s}{\partial y^2} \tag{10}$$

$$\varepsilon_z = 0 \tag{11}$$

$$\gamma_{xy} = -2z\frac{\partial^2 w_b}{\partial x \partial y} - f(z)\frac{\partial^2 w_s}{\partial x \partial y} \tag{12}$$

$$\gamma_{yz} = g(z)\frac{\partial w_s}{\partial y} \tag{13}$$

$$\gamma_{xz} = g(z)\frac{\partial w_s}{\partial x} \tag{14}$$

where

$$g(z) = 1 - \frac{df(z)}{dz} = \frac{5}{4} - 5\left(\frac{z}{h}\right)^2 \tag{15}$$

Substituting strains from Eqs. (9)-(14) in constitutive equations (3), one obtains the expressions for stresses:

$$\sigma_x = -\frac{Ez}{1-\mu^2}\left(\frac{\partial^2 w_b}{\partial x^2} + \mu\frac{\partial^2 w_b}{\partial y^2}\right) - \frac{E}{1-\mu^2}f(z)\left(\frac{\partial^2 w_s}{\partial x^2} + \mu\frac{\partial^2 w_s}{\partial y^2}\right) \tag{16}$$

$$\sigma_y = -\frac{Ez}{1-\mu^2}\left(\frac{\partial^2 w_b}{\partial y^2} + \mu\frac{\partial^2 w_b}{\partial x^2}\right) - \frac{E}{1-\mu^2}f(z)\left(\frac{\partial^2 w_s}{\partial y^2} + \mu\frac{\partial^2 w_s}{\partial x^2}\right) \tag{17}$$

$$\tau_{xy} = -\frac{Ez}{1+\mu}\frac{\partial^2 w_b}{\partial x \partial y} - \frac{E}{1+\mu}f(z)\frac{\partial^2 w_s}{\partial x \partial y} \tag{18}$$

$$\tau_{yz} = \frac{E}{2(1+\mu)}g(z)\frac{\partial w_s}{\partial y} \tag{19}$$

$$\tau_{zx} = \frac{E}{2(1+\mu)}g(z)\frac{\partial w_s}{\partial x} \tag{20}$$

The moments and shear forces are defined as:

$$\begin{aligned}
(M_x^b, M_y^b, M_{xy}^b) &= \int_{-h/2}^{h/2} (\sigma_x, \sigma_y, \tau_{xy}) z dz \\
(M_x^s, M_y^s, M_{xy}^s) &= \int_{-h/2}^{h/2} (\sigma_x, \sigma_y, \tau_{xy}) f(z) dz \\
(Q_{xz}^s, Q_{yz}^s) &= \int_{-h/2}^{h/2} (g(z)\tau_{xz}, g(z)\tau_{yz}) dz
\end{aligned} \tag{21}$$

Substituting stress components in Eq. (21), one obtains the moments and shear forces:

$$M_x^b = -D^b\left(\frac{\partial^2 w_b}{\partial x^2} + \mu\frac{\partial^2 w_b}{\partial y^2}\right) \tag{22}$$

$$M_y^b = -D^b\left(\frac{\partial^2 w_b}{\partial y^2} + \mu\frac{\partial^2 w_b}{\partial x^2}\right) \tag{23}$$

$$M_{xy}^b = -D^b(1-\mu)\frac{\partial^2 w_b}{\partial x \partial y} \tag{24}$$

$$M_x^s = -D^s\left(\frac{\partial^2 w_s}{\partial x^2} + \mu\frac{\partial^2 w_s}{\partial y^2}\right) \tag{25}$$

$$M_y^s = -D^s\left(\frac{\partial^2 w_s}{\partial y^2} + \mu\frac{\partial^2 w_s}{\partial x^2}\right) \tag{26}$$

$$M_{xy}^s = -D^s(1-\mu)\frac{\partial^2 w_s}{\partial x \partial y} \tag{27}$$

$$Q_x^s = D^Q\frac{\partial w_s}{\partial x} \tag{28}$$

$$Q_y^s = D^Q\frac{\partial w_s}{\partial y} \tag{29}$$

where

$$D^b = \frac{E}{(1-\mu^2)}\int_{-h/2}^{h/2} z^2 dz\,, \quad D^s = \frac{E}{(1-\mu^2)}\int_{-h/2}^{h/2} (f(z))^2 dz\,, \quad D^Q = \frac{5Eh}{12(1+\mu)} \tag{30}$$

2.3. Governing equations

The virtual work equation leads to:

$$\int\left[M_x^b\delta\kappa_x^b + M_y^b\delta\kappa_y^b + M_{xy}^b\delta\kappa_{xy}^b\right]dA = \int\left[q - k_f(w_b + w_s)\right]\delta w_b dA \tag{31}$$

$$\begin{aligned}\int\left[M_x^s\delta\kappa_x^s + M_y^s\delta\kappa_y^s + M_{xy}^s\delta\kappa_{xy}^s\right]dA + \int\left[Q_y^s\delta w_{s,y} + Q_x^s\delta w_{s,x}\right]dA = \\ = \int\left[q - k_f(w_b + w_s)\right]\delta w_s dA\end{aligned} \tag{32}$$

where k_f is modulus of elastic foundation and also:

$$\begin{aligned}&\kappa_x^b = \frac{\partial^2 w_b}{\partial x^2}, \quad \kappa_y^b = \frac{\partial^2 w_b}{\partial y^2}, \quad \kappa_{xy}^b = \frac{\partial^2 w_b}{\partial x \partial y}, \quad \kappa_x^s = \frac{\partial^2 w_s}{\partial x^2},\\ &\kappa_y^s = \frac{\partial^2 w_s}{\partial y^2}, \quad \kappa_{xy}^s = \frac{\partial^2 w_s}{\partial x \partial y}\end{aligned} \tag{33}$$

Substituting Eqs. (9)-(14) into Eqs. (31)-(32), one will obtain the following governing equations:

$$\begin{aligned}&\delta w_b : \frac{\partial^2 M_x^b}{\partial x^2} + 2\frac{\partial^2 M_{xy}^b}{\partial x \partial y} + \frac{\partial^2 M_y^b}{\partial y^2} + q - k_f(w_b + w_s) = 0\\ &\delta w_s : \frac{\partial^2 M_x^s}{\partial x^2} + 2\frac{\partial^2 M_{xy}^s}{\partial x \partial y} + \frac{\partial^2 M_y^s}{\partial y^2} + \frac{\partial Q_{xz}^s}{\partial x} + \frac{\partial Q_{yz}^s}{\partial y} + q - k_f(w_b + w_s) = 0\end{aligned} \tag{34}$$

Beside the above equations, the remaining terms describe the boundary conditions. Finally, by substituting Eqs. (22)-(29), into Eqs. (34), two coupled partial differential equations as governing equations of rectangular plate resting on Winkler elastic foundation will be obtained:

$$D\nabla^2\nabla^2 w_b = q - k_f(w_b + w_s) \tag{35}$$

$$\frac{1}{84}D\nabla^2\nabla^2 W_s - \frac{5Eh}{12(1+\nu)}\nabla^2 w_s = q - k_f(w_b + w_s) \tag{36}$$

where D is the flexural rigidity of plate that can be defined as:

$$D = \frac{Eh^3}{12(1-\mu^2)} \tag{37}$$

The boundary conditions for simply supported plate are given as below:

$$x = 0, a: \quad w_b = 0, \quad M_x^b = 0, \quad w_s = 0, \quad M_x^s = 0 \tag{38}$$

$$y = 0, b: \quad w_b = 0, \quad M_y^b = 0, \quad w_s = 0, \quad M_y^s = 0 \tag{39}$$

The boundary conditions for clamped edge are given as Eq. (40) and (41).

$$x = 0, a: \quad w_b = 0, \quad \frac{\partial w_b}{\partial x} = 0, \quad w_s = 0, \quad \frac{\partial w_s}{\partial x} = 0 \tag{40}$$

$$y = 0, b: \quad w_b = 0, \quad \frac{\partial w_b}{\partial y} = 0, \quad w_s = 0, \quad \frac{\partial w_s}{\partial y} = 0 \tag{41}$$

The boundary conditions for free edge are given as below:

$$x = 0, a \rightarrow \begin{cases} M_x^b = 0, & -D^b\left[\dfrac{\partial^3 w_b}{\partial x^3} + (2-\mu)\dfrac{\partial^3 w_b}{\partial x \partial y^2}\right] = 0 \\ M_x^s = 0, & \dfrac{420(1-\mu)D^b}{h^2}\dfrac{\partial w_s}{\partial x} - D^b\left[\dfrac{\partial^3 w_s}{\partial x^3} + (2-\mu)\dfrac{\partial^3 w_s}{\partial x \partial y^2}\right] = 0 \end{cases} \tag{42}$$

$$y = 0, b \rightarrow \begin{cases} M_y^b = 0, & -D^b\left[\dfrac{\partial^3 w_b}{\partial y^3} + (2-\mu)\dfrac{\partial^3 w_b}{\partial y \partial x^2}\right] = 0 \\ M_y^s = 0, & \dfrac{420(1-\mu)D^b}{h^2}\dfrac{\partial w_s}{\partial y} - D^b\left[\dfrac{\partial^3 w_s}{\partial y^3} + (2-\mu)\dfrac{\partial^3 w_s}{\partial y \partial x^2}\right] = 0 \end{cases} \tag{43}$$

3. The Navier Solution

The governing equations (35) and (36) are coupled and cannot be solved independently. The Navier method is adopted for solving this problem. This method has been presented for solution of bending of simply supported plates by double trigonometric series [28]. The solution of the governing differential equations (35) and (36), have to be sought in the form of infinite Fourier series, as follows:

$$w_b(x,y) = \sum_{m=1}^{\infty}\sum_{n=1}^{\infty} w_{mn}^b \sin\left(\frac{m\pi x}{a}\right)\sin\left(\frac{n\pi y}{b}\right) \tag{44}$$

$$w_s(x,y) = \sum_{m=1}^{\infty}\sum_{n=1}^{\infty} w_{mn}^s \sin\left(\frac{m\pi x}{a}\right)\sin\left(\frac{n\pi y}{b}\right) \tag{45}$$

It can be easily verified that these expression for deflections automatically satisfy the boundary conditions (38) and (39). Also the general load $q(x, y)$ can be approximated as following double Fourier expansion equation:

$$q(x,y) = \sum_{m=1}^{\infty}\sum_{n=1}^{\infty} q_{mn} \sin\left(\frac{m\pi x}{a}\right)\sin\left(\frac{n\pi y}{b}\right) \tag{46}$$

The coefficients q_{mn} are calculated as [22]:

$$q_{mn} = \frac{4}{ab}\int_0^a\int_0^b q(x,y)\sin\frac{m\pi x}{a}\sin\frac{n\pi y}{b}dxdy \tag{47}$$

Substituting Eqs. (44)-(47) into Eqs. (35) and (36), the following equations will be obtained:

$$\left\{D\left[\left(\frac{m\pi}{a}\right)^2+\left(\frac{n\pi}{b}\right)^2\right]^2+k_f\right\}w_{mn}^b + k_f w_{mn}^s = q_{mn} \tag{48}$$

$$\left\{\frac{D}{84}\left[\left(\frac{m\pi}{a}\right)^2+\left(\frac{n\pi}{b}\right)^2\right]^2+\frac{5Gh}{6}\left[\left(\frac{m\pi}{a}\right)^2+\left(\frac{n\pi}{b}\right)^2\right]+k_f\right\}w_{mn}^s + k_f w_{mn}^b = q_{mn} \tag{49}$$

The coefficients w_{mn}^b and w_{mn}^s are determined by solving above equations:

$$w_{mn}^b = \frac{\left(\frac{D}{84}B^2+\frac{5}{6}GhB\right)q_{mn}}{A} \tag{50}$$

$$w^s_{mn} = \frac{DB^2 q_{mn}}{A} \tag{51}$$

where A and B are:

$$A = \frac{1}{84}D^2B^4 + \frac{5}{6}DGhB^3 + \frac{85}{84}k_f DB^2 + \frac{5}{6}k_f GhB \tag{52}$$

$$B = \left[\left(\frac{m\pi}{a}\right)^2 + \left(\frac{n\pi}{b}\right)^2\right] \tag{53}$$

If the plate does not rest on elastic foundation, the governing equations (35) and (36) will be uncoupled and the coefficients w^b_{mn} and w^s_{mn} will be simply determined as the Eqs. (54) and (55):

$$w^b_{mn} = \frac{q_{mn}}{D\pi^4(m^2/a^2 + n^2/b^2)^2} \tag{54}$$

$$w^s_{mn} = \frac{q_{mn}}{\frac{D\pi^4}{84}(m^2/a^2 + n^2/b^2)^2 + \frac{5Eh\pi^2}{12(1+\mu)}(m^2/a^2 + n^2/b^2)} \tag{55}$$

4. Results and Discussions

For the purpose of presenting the results, the following non-dimensional parameters are introduced:

$$\bar{w} = \frac{100Eh^3}{q_0 a^4}w \quad \text{(for problems without elastic foundation)} \tag{56}$$

$$\bar{w} = \frac{1000D}{q_0 a^4}w \quad \text{(for problems with elastic foundation)} \tag{57}$$

$$\left(\bar{\sigma}_x, \bar{\sigma}_y, \bar{\tau}_{xy}\right) = \frac{\left(\sigma_x, \sigma_y, \tau_{xy}\right)}{100q_0} \tag{58}$$

$$\left(\bar{\tau}_{xz}, \bar{\tau}_{yz}\right) = \frac{\left(\bar{\tau}_{xz}, \bar{\tau}_{yz}\right)}{10q_0} \tag{59}$$

$$\left(\bar{M}_x, \bar{M}_y, \bar{M}_{xy}\right) = \left(M_x, M_y, M_{xy}\right)\frac{100}{q_0 a^2} \tag{60}$$

$$\left(\bar{Q}_x, \bar{Q}_y\right) = \frac{\left(Q_x, Q_y\right)}{q_0 a} \tag{61}$$

$$K = \left(\frac{k_f a^4}{D}\right)^{0.25} \tag{62}$$

where q_0 is the maximum lateral load intensity in each problem.

In sequel, some typical benchmark problems will be solved by the two--variable refined plate theory (RPT) and the obtained results will be compared with other plate theories and the exact solution. The sketches of these problems are shown in Figs. 2 and 3. Exact solutions of these problems exist in the literature and that is one of the main reasons of choosing them as benchmark problems. Also, these problems have physical interpretation in engineering applications; for example contact loading can be simulated by uniform and sinusoidal loading and hydrostatic pressure can be simulated by linear loading. As it is mentioned in Introduction, many problems of considerable practical importance can be related to the solution of plates resting on an elastic foundation. The exact solution is used as a basis for comparison of results and the percentage error is defined as below:

$$\%\text{error} = \frac{\text{value by each theory} - \text{exact value}}{\text{exact value}} \times 100 \tag{63}$$

In each example, the percentage error is shown in parenthesis in subsequent tables. The plate material properties in all following benchmark problems are considered as: $E = 210$ GPa and $\mu = 0.3$.

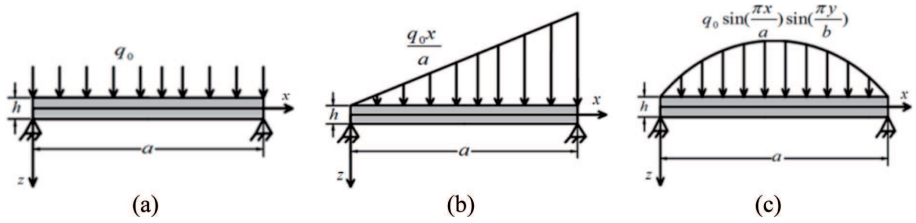

Fig. 2. Simply supported rectangular plates subjected to (a) uniform loading (b) linear loading; (c) sinusoidal loading

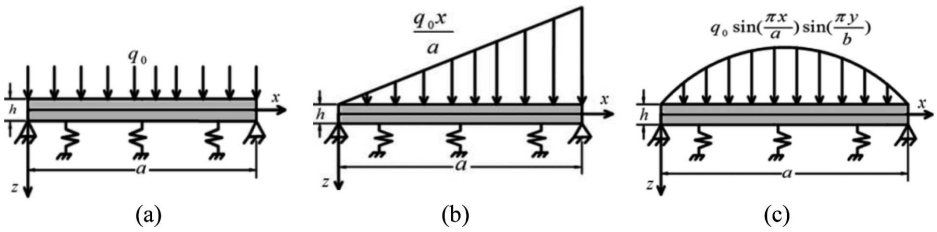

Fig. 3. Simply supported rectangular plates resting on elastic foundation subjected to (a) uniform loading (b) linear loading; (c) sinusoidal loading

Example 1: Consider a rectangular plate (of length a, width b and thickness h) subjected to uniformly distributed transverse load q_0, acting in z direction as illustrated in Fig. 2a. According to Eq. (47), the coefficients q_{mn} are calculated as:

$$q_{mn} = \frac{16q_0}{\pi^2 mn} m, n = 1, 3, 5, ... \tag{64}$$

where q_0 is the intensity of uniform loading. After computing coefficients w^b_{mn} and w^b_{mn} by Eqs. (54) and (55), the deflections, strains and stresses will be determined through Eqs. (6)-(20). The obtained results are listed in Table 1.

The obtained displacement by RPT is very close to HSDT, FSDT and TSDT; where all these theories give excellent results with respect to exact solution. A brief resume of assumptions and equations of plate theories used for comparison are given in the Appendix. This issue is seen for values of in-plane normal stresses too. Also the values of in-plane shear stresses obtained by RPT are in excellent agreement with the results of other theories.

Table 1.
Comparison of deflection $\bar{w}$ at (a/2, b/2, 0), in-plane normal stresses $\bar{\sigma}_x$ and $\bar{\sigma}_y$ at (a/2, b/2, h/2) and in-plane shear stress $\bar{\tau}_{xy}$ at (0, 0, h/2) in rectangular isotropic plate subjected to uniformly distributed loading (a/b = 0.5 and h/a = 0.1)

Theory	$\bar{w}$	$\bar{\sigma}_x$	$\bar{\sigma}_y$	$\bar{\tau}_{xy}$	$\bar{\tau}_{xz}$
Present	11.41 (0.35)	0.612 (0.00)	0.279 (–0.71)	0.280	0.679 (0.00)
TSDT [27]	11.34 (–0.26)	0.638 (4.25)	0.245 (–12.81)	0.277	0.701 (3.24)
HSDT [4]	11.42 (0.44)	0.612 (0.00)	0.278 (–1.07)	0.280	0.679 (0.00)
FSDT [2]	11.42 (0.44)	0.610 (–0.33)	0.277 (–1.42)	0.276	0.545 (–19.73)
CPT [1]	11.06 (–2.73)	0.610 (–0.33)	0.278 (–1.07)	0.277	–
EXACT [6]	11.37	0.612	0.281	–	0.679

Example 2: Consider previous rectangular plate which is subjected to linearly distributed loading as shown in Fig. 2b. Using Eq. (47), the coefficient of Fourier expansion can be calculated as:

$$q_{mn} = \frac{8q_0}{\pi^2 mn} \cos m\pi \tag{65}$$

The obtained results are compared with other theories in Table 2 and Table 3 for a/b = 1 and a/b = 0.5 respectively. The central deflections predicted by RPT have good agreement with the exact values. The obtained deflections values are predicted only 0.58% and 0.36% more than the exact value for square and rectangular plates respectively. The in–plane normal

Table 2.
Comparison of deflection $\bar{w}$ at (a/2, b/2, 0), in-plane normal stresses $\bar{\sigma}_x$ and $\bar{\sigma}_y$ at (a/2, b/2, h/2) and in-plane shear stress $\bar{\tau}_{xy}$ at (0, 0, h/2) in square isotropic plate subjected to linear transverse loading. (a/b = 1 and h/a = 0.1)

Theory	$\bar{w}$	$\bar{\sigma}_x$	$\bar{\sigma}_y$	$\bar{\tau}_{xy}$
Present (RPT)	2.3329 (0.58)	0.1445 (0.00)	0.1445 (0.00)	0.0873
TSDT [27]	2.3125 (–0.30)	0.1535 (6.23)	0.1535 (6.23)	0.0975
HSDT [4]	2.3325 (0.56)	0.1445 (0.00)	0.1445 (0.00)	0.0995
FSDT [2]	2.3350 (0.67)	0.1435 (–0.7)	0.1435 (–0.7)	0.0975
CPT [1]	2.2180 (–4.38)	0.1435 (–0.7)	0.1435 (–0.7)	0.0975
EXACT [6]	2.3195	0.1445	0.1445	–

Table 3.
Comparison of deflection $\bar{w}$ at (a/2, b/2, 0), in-plane normal stresses $\bar{\sigma}_x$ and $\bar{\sigma}_y$ at (a/2, b/2, h/2), in-plane shear stress $\bar{\sigma}_{xy}$ at (0, 0, h/2) and transverse shear stress $\bar{\sigma}_{xz}$ at (0, b/2, 0) in rectangular isotropic plate subjected to linear transverse loading (a/b = 0.5 and h/a = 0.1)

Theory	$\bar{w}$	$\bar{\sigma}_x$	$\bar{\sigma}_y$	$\bar{\tau}_{xy}$
Present	5.7078 (0.357)	0.3063 (0.098)	0.1396 (0.64)	0.1612
TSDT [27]	5.6700 (–0.307)	0.3194 (4.379)	0.1125 (–19.93)	0.1385
HSDT [4]	5.7100 (0.396)	0.3060 (0.00)	0.1390 (–1.067)	0.1400
FSDT [2]	5.7100 (0.396)	0.3048 (–0.392)	0.1385 (–1.42)	0.1380
CPT [1]	5.5300 (–2.769)	0.3048 (–0.392)	0.1390 (–1.067)	0.1385
EXACT [6]	5.6875	0.3060	0.1405	–

stresses are in good agreement with the exact solution and other refined theories for both square and rectangular plates. For the square plate, the obtained in–plane normal stresses exactly coincide on the exact solution. The obtained in–plane shear stresses by RPT and other theories are in same range. The distribution of transverse shear stresses across the thickness is parabolically as expected and shown in Fig. 4. It must be noted that the transverse shear stresses shown in Fig. 4 are obtained by constitutive relations where they can be determined by equilibrium equations too.

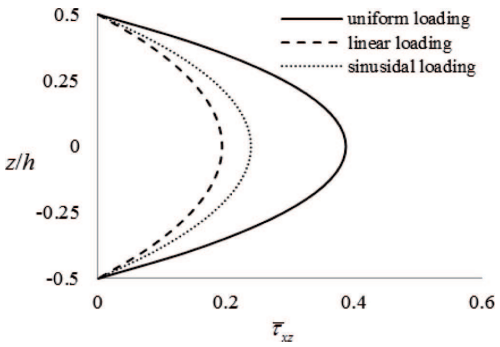

Fig. 4. The parabolic variation of out of plane shear stress in z-direction for various loading ($a/b = 1$, $h/a = 0.1$)

Example 3: As illustrated in Fig. 3c, the sinusoidally distributed load in both x and y directions are applied on the simply supported rectangular plate. The distributed load is expressed as:

$$q(x, y) = q_0 \sin\left(\frac{\pi x}{a}\right) \sin\left(\frac{\pi y}{b}\right) \tag{66}$$

As it can be seen in Table 4, the obtained deflections by the RPT have good agreement with the exact solution and other theories. The obtained transverse shear stress is identical to the exact solution for this kind of loading. Also the in–plane shear stresses are in a same range for all theories.

Table 4.
Comparison of deflection $\bar{w}$ at ($a/2$, $b/2$, 0), in–plane shear stress $\bar{\tau}_{xy}$ at (0, 0, $h/2$) and transverse shear stress $\bar{\tau}_{xz}$ at (0, $b/2$, 0) in square isotropic plate subjected to sinusoidally distributed loading ($a/b = 1$ and $h/a = 0.1$)

Theory	$\bar{w}$	$\bar{\tau}_{xy}$	$\bar{\tau}_{xz}$
Present	2.960 (0.61)	0.105	0.238 (0.00)
TSDT [27]	2.933 (–0.30)	0.110	0.245 (2.94)
HSDT [4]	2.960 (0.61)	0.107	0.238 (0.00)
FSDT [2]	2.934 (0.27)	0.106	0.169 (–29.0)
CPT [1]	2.802 (–4.76)	0.106	–
EXACT [6]	2.942	–	0.238

One of the Advantages of the RPT, as mentioned before, is that it can predict parabolic transverse shear stresses such that the condition of free traction is satisfied on plate surfaces and also the shear correction factor is not

required. As shown in Fig. 4, the transverse shear stress varies parabolically across the plate thickness and it comes to zero at plate surfaces for all applied loadings.

The obtained results in these three examples show the good performance of the RPT in modeling flexure of thick plates. In sequel, this theory will be adopted for modeling thick plates resting on Winkler elastic foundation. Different loading conditions are considered and the effects of foundation modulus, plate thickness and type of loading will be studied.

Example 4: In this example a simply supported square plate resting on Winkler foundation is subjected to a uniformly distributed transverse loading as shown in Fig. 3a. The coefficients of double Fourier expansion of uniform loading were presented in Eq. (64).

The obtained non–dimensional deflections, moments and shear forces are compared with the CPT and FSDT results in Table 5. Although the results obtained by the RPT and FSDT are very close, the CPT predicts deflections and moments slightly different from them. In Table 6 the effects of plate thickness and foundation modulus on deflections, moments and resultant transverse forces are investigated. Again, the results show that predicted values for RPT and FSDT are very close together and in many cases are identical. For $h/a = 0.2$, the effect of elastic foundation on the deflections of plate is shown in the Fig. 5. As shown in this figure, the deflections are decreased by increasing the foundation stiffness.

Table 5.
Comparison of non–dimensional deflections, moments and shear forces at ($x = a/2$, $y = b/2$) in square isotropic plates subjected to uniform loading and resting on elastic foundation ($a/b = 1$ and $h/a = 0.05$)

Theory	$\bar{w}$ (at $z = 0$)	$\bar{M}_x$	$\bar{M}_y$	$\bar{M}_{xy}$	$\bar{Q}_x$	$\bar{Q}_y$
(1) $K = 1$						
Present	4.106	4.783	4.783	3.240	0.332	–0.332
CPT	4.053	4.809	4.809	2.943	–	–
FSDT	4.104	4.775	4.775	3.241	0.337	–0.337
(2) $K = 3$						
Present	3.381	3.865	3.865	2.745	0.288	–0.288
CPT	3.348	3.910	3.910	2.456	–	–
FSDT	3.381	3.865	3.865	2.746	0.292	–0.292
(3) $K = 5$						
Present	1.509	1.525	1.525	1.451	0.171	–0.171
CPT	1.507	1.575	1.575	1.181	–	–
FSDT	1.509	1.526	1.529	1.452	0.175	–0.175

Table 6.
Non-dimensional deflections, moments and shear forces in square isotropic plates subjected to uniform loading and resting on elastic foundation ($a/b = 1$). Deflections and moments at ($x = a/2$, $y = b/2$), $\bar{Q}_x$ at ($x = 0$, $y = a/2$) and $\bar{Q}_y$ at ($x = a/2$, $y = a$)

h/a		$\bar{w}$ (at $z = 0$)	$\bar{M}_x$	$\bar{M}_y$	$\bar{M}_{xy}$	$\bar{Q}_x$	$\bar{Q}_y$
(1) $K = 1$							
0.01	Present	4.054	4.775	4.775	3.240	0.333	–0.333
	FSDT	4.054	4.775	4.775	3.241	0.337	–0.337
0.05	Present	4.104	4.775	4.775	3.241	0.333	–0.337
	FSDT	4.104	4.775	4.775	3.241	0.337	–0.337
0.1	Present	4.261	4.774	4.774	3.240	0.330	–0.330
	FSDT	4.261	4.774	4.774	3.240	0.337	–0.337
0.2	Present	4.887	4.772	4.772	3.238	0.325	–0.325
	FSDT	4.888	4.772	4.772	3.239	0.337	–0.337
(2) $K = 3$							
0.01	Present	3.348	3.875	3.875	2.750	0.289	–0.289
	FSDT	3.349	3.875	3.875	2.751	0.293	–0.293
0.05	Present	3.381	3.865	3.865	2.745	0.288	–0.288
	FSDT	3.381	3.865	3.865	2.746	0.292	–0.292
0.1	Present	3.483	3.834	3.834	2.727	0.284	–0.284
	FSDT	3.483	3.834	3.834	2.728	0.291	–0.291
0.2	Present	3.873	3.716	3.716	2.659	0.279	–0.279
	FSDT	3.873	3.716	3.716	2.660	0.284	–0.284
(3) $K = 5$							
0.01	Present	1.506	1.540	1.540	1.461	0.173	–0.173
	FSDT	1.506	1.540	1.540	1.462	0.176	–0.176
0.05	Present	1.509	1.525	1.525	1.451	0.171	–0.171
	FSDT	1.509	1.526	1.526	1.452	0.175	–0.175
0.1	Present	1.519	1.481	1.481	1.372	0.159	–0.159
	FSDT	1.519	1.482	1.482	1.421	0.172	–0.172
0.2	Present	1.551	1.328	1.328	1.311	0.151	–0.151
	FSDT	1.551	1.328	1.328	1.311	0.162	–0.162

According to Eqn. (44) and (45), the deflections and consequently stresses and stress resultants are calculated by some double trigonometric series.

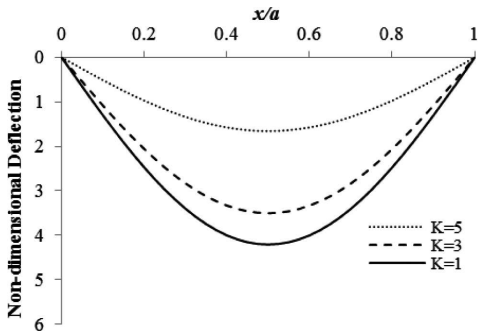

Fig. 5. The effect of foundation modulus on non-dimensional deflections of simply supported square plates subjected to uniformly distributed loading (h/a = 0.2)

Proper number of terms should be used for convergence of these series. In Table 7, the effect of number of terms on convergence of deflection, resultant force and moment is investigated. The previous square plate resting on elastic foundation and subjected to uniform loading is studied. Although the deflection converges for m, n = 11, the stress resultants and couples converge by considering more terms. Since the stress resultants and couples are obtained from the second and third derivatives of the deflection, this issue is predictable [22]. It must be noted that the converged results are presented in all examples.

Table 7.
Convergence study for square plate resting on elastic foundation and subjected to uniform loading (a/b = 1, h/a = 0.2, K = 1)

	$m, n = 1$	$m, n = 5$	$m, n = 10$	$m, n = 11$	$m, n = 12$	$m, n = 17$	$m, n = 20$
$\bar{w}$	5.080	4.893	4.888	4.887	4.887	4.887	4.887
$\bar{Q}_x$	0.256	0.304	0.314	0.316	0.316	0.321	0.325
$\bar{M}_x$	5.321	4.806	4.780	4.767	4.767	4.773	4.772

Example 5: According to Fig. 3b, a simply supported square plate resting on elastic foundation is subjected to linearly distributed loading on $z = -h/2$. The effect of thickness and foundation modulus are studied and the obtained results are listed in Table 8. The deflections, moments and shear forces are decreased by increasing the foundation modulus. Considering different values of foundation modulus, the deflections of points lying on x-axis are plotted in Fig. 6. Since the loading varies linearly, the obtained deflections are not symmetric and the maximum deflection does not take place at center of plate. It can be seen the deflection profile moves toward symmetric behavior when the foundation modulus is decreased.

Table 8.

Non-dimensional deflections, moments and shear forces in square plate subjected to linear transverse loading and resting on elastic foundation; $\bar{w}$ and $\bar{M}_x$ at ($x = a/2$, $y = b/2$), $\bar{M}_{xy}$ at ($x = 0$, $y = a$), $\bar{Q}_x$ at ($x = 0$, $y = a/2$) and $\bar{Q}_y$ at ($x = a/2$, $y = a$)

h/a	$\bar{w}$ (at $z = 0$)	$\bar{M}_x$	$\bar{M}_y$	$\bar{M}_{xy}$	$\bar{Q}_x$	$\bar{Q}_y$
(1) $K = 1$						
0.01	2.027	2.387	2.387	1.109	0.089	–0.089
0.02	2.030	2.387	2.387	1.109	0.089	–0.089
0.05	2.052	2.387	2.387	1.109	0.089	–0.089
0.1	2.130	2.387	2.387	1.109	0.089	–0.089
0.15	2.260	2.386	2.386	1.109	0.089	–0.089
0.2	2.443	2.386	2.386	1.109	0.089	–0.089
(2) $K = 3$						
0.01	1.674	1.937	1.937	0.879	0.069	–0.069
0.02	1.676	1.936	1.936	0.878	0.069	–0.069
0.05	1.690	1.932	1.932	0.876	0.068	–0.068
0.1	1.741	1.917	1.917	0.869	0.068	–0.068
0.15	1.824	1.892	1.892	0.857	0.067	–0.067
0.2	1.936	1.858	1.858	0.841	0.065	–0.065
(3) $K = 5$						
0.01	0.753	0.769	0.769	0.309	0.019	–0.019
0.02	0.753	0.769	0.769	0.309	0.019	–0.019
0.05	0.754	0.762	0.762	0.306	0.019	–0.019
0.1	0.759	0.740	0.740	0.298	0.019	–0.019
0.15	0.766	0.706	0.706	0.286	0.018	–0.018
0.2	0.775	0.663	0.663	0.270	0.017	–0.017

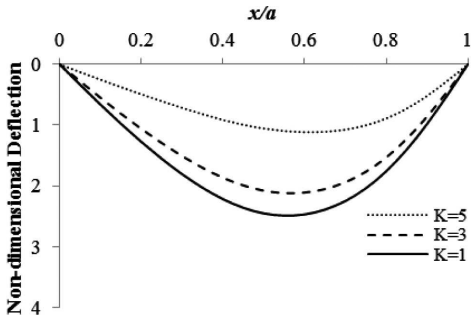

Fig. 6. The effect of foundation modulus on non–dimensional deflections of simply supported square plates subjected to linearly distributed loading ($h/a = 0.2$)

Example 6: As shown in Fig. 3c, a simply supported square plate resting on elastic foundation is subjected to sinusoidal loading in both x and y directions. Similar to pervious example the effect of thickness and foundation stiffness are studied and the results are shown in Table 9 and Fig. 7. According to Table 9, the deflections, moments and shear forces are decreased by increasing the foundation modulus. This issue is seen also in Fig. 7 where the deflections are decreased by foundation stiffness increase. Since the loading is symmetric, the deflections are obtained symmetric too.

Table 9.

Non-dimensional deflections, moments and shear forces in square isotropic plates subjected to sinusoidal loading and resting on elastic foundation. Deflections and moments at ($x = a/2$, $y = b/2$), $\bar{Q}_x$ at ($x = 0$, $y = a/2$) and $\bar{Q}_y$ at ($x = a/2$, $y = a$)

h/a	$\bar{w}$ (at $z = 0$)	$\bar{M}_x$	$\bar{M}_y$	$\bar{M}_{xy}$	$\bar{Q}_x$	$\bar{Q}_y$
(1) $K = 1$						
0.01	2.561	3.284	3.284	1.768	0.158	–0.158
0.02	2.565	3.284	3.284	1.768	0.158	–0.158
0.05	2.596	3.284	3.284	1.768	0.158	–0.158
0.1	2.703	3.284	3.284	1.768	0.158	–0.158
0.15	2.883	3.283	3.283	1.768	0.158	–0.158
0.2	3.134	3.282	3.282	1.768	0.158	–0.158
(2) $K = 3$						
0.01	2.126	2.726	2.726	1.468	0.132	–0.132
0.02	2.128	2.725	2.725	1.467	0.131	–0.131
0.05	2.149	2.719	2.719	1.464	0.131	–0.131
0.1	2.223	2.700	2.700	1.454	0.130	–0.130
0.15	2.343	2.668	2.668	1.436	0.128	–0.128
0.2	2.506	2.624	2.624	1.413	0.126	–0.126
(3) $K = 5$						
0.01	0.985	1.264	1.264	0.680	0.061	–0.061
0.02	0.986	1.263	1.263	0.680	0.061	–0.061
0.05	0.990	1.253	1.253	0.675	0.060	–0.060
0.1	1.006	1.222	1.222	0.658	0.059	–0.059
0.15	1.030	1.173	1.173	0.631	0.056	–0.056
0.2	1.060	1.110	1.110	0.598	0.053	–0.053

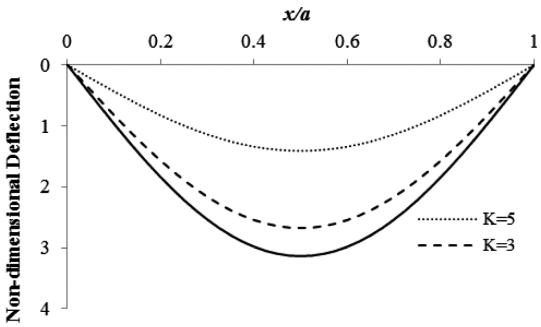

Fig. 7. The effect of foundation modulus on non-dimensional deflections of simply supported square plates subjected to sinusoidally distributed loading (h/a = 0.2)

Finally, the effect of thickness on central deflection of square plate resting on elastic foundation for different loading conditions is studied. As shown in Fig. 8, the central deflections are decreased by increasing the plate thickness for all types of loadings. Considering same q_0 for all types of loadings, as expected the central deflection for uniform loading is obtained more than sinusoidal and linear loadings; and among the sinusoidal and linear loadings, the obtained central deflections of the former are greater than the latter.

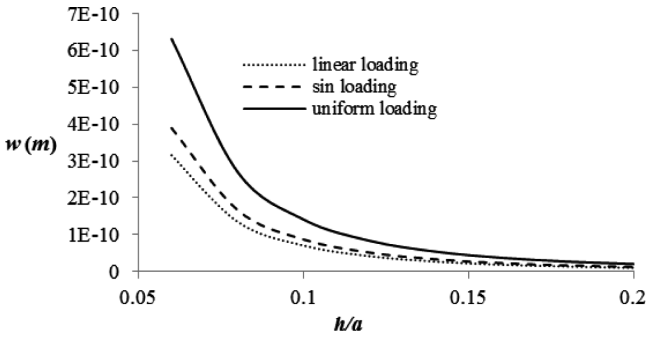

Fig. 8. The effect of thickness on central deflection of square plates by different type of loading. (k_f = 20 kN/m^2· m)

5. Conclusions

The two–variable refined plate theory (RPT) was used in this paper for the analysis of moderately thick plates resting on elastic foundation subjected to various types of loadings. This theory contains only two unknown parameters, predicts parabolic transverse shear stresses such that the condition of free traction is satisfied and does not need the shear correction factor. It gives excellent results compared to other common theories and also it is relatively easy to apply. Several benchmark problems were studied and the

obtained results were compared with other plate theories, and exact solutions and capability of present theory in modeling these problems was proved.

Also the effects of foundation modulus, plate thickness and type of loading on obtained results were studied. The deflections, moments and shear forces were decreased by increasing the foundation modulus and plates thickness. The transverse shear stresses varied parabolically across the plate thickness and it satisfied the zero traction on the plate surfaces.

Appendixes

Classical plate theory (CPT):

The CPT is the simplest theory of plate that gives good results for thin plates but cannot predict the transverse shear stresses along the thickness. The main assumptions of this theory are as below:

- The line which is perpendicular to middle surface remains line after deflection.
- The line which is perpendicular to middle surface remains perpendicular to it after deflection.
- The normal stress in direction of plate thickness is neglected.

The displacement field based on this theory can be determined as below:

$$\begin{aligned} u(x,y,z) &= -z\frac{\partial w}{\partial x} \\ v(x,y,z) &= -z\frac{\partial w}{\partial y} \\ w(x,y,z) &= w_0(x,y) \end{aligned} \tag{67}$$

where w is the only unknown parameter in this theory.

First-order shear deformation plate theory (FSDT):

The FSDT predicts the constant transverse shear stress along the plate thickness which is not consistent with zero stress conditions on free surfaces. In this theory, the shear correction factor is needed to modify the value of maximum shear stress with that of exact value. Assumptions of this theory are as below:

- The line which is perpendicular to middle surface remains line after deflection.
- The line which is perpendicular to middle surface doesn't remain perpendicular to it after deflection.
- The normal stress in direction of plate thickness is neglected.

The displacement field based this theory is as below:

$$\begin{aligned} u(x,y,z) &= z\phi_x(x,y) \\ v(x,y,z) &= z\phi_y(x,y) \\ w(x,y,z) &= w_0(x,y) \end{aligned} \tag{68}$$

where ϕ_x, ϕ_x and w_0 are the unknown parameter in this theory.

Higher-order shear deformation plate theory (HSDT):

The HSDTs were developed in order to eliminate the defects of FSDT. There are many kinds of this theory based on the number of unknown parameter. For example the third-order shear deformation theory of Reddy is constructed based of following assumptions:

– The line which is perpendicular to middle surface doesn't remain line after deflection.
– The line which is perpendicular to middle surface doesn't remain perpendicular to it after deflection.
– The normal stress in direction of plate thickness is neglected.

The displacement field of this theory is obtained as below:

$$\begin{aligned} u(x,y,z) &= z\phi_x(x,y) + z^2\theta_x(x,y) + z^3\lambda_x(x,y) \\ v(x,y,z) &= z\phi_y(x,y) + z^2\theta_y(x,y) + z^3\lambda_y(x,y) \\ w(x,y,z) &= w_0(x,y) \end{aligned} \tag{69}$$

where ϕ_x, ϕ_y, θ_x, θ_x, λ_x and λ_y are the unknown parameter in this theory.

Trigonometric shear deformation plate theory (TSDT):

The TSDT included four unknown parameter and consider the shear deformation effects. Assumptions of this theory are as below:

– Displacements are small in comparison with the plate thickness.
– The line which is perpendicular to middle surface doesn't remain line after deflection.
– The in-plane displacements consist of two parts: a component analogous to bending displacement in classical plate theory and second component due to shear deformation which is assumed to be sinusoidal in nature with respect to thickness coordinate.
– The normal stress in direction thickness is zero.

The displacement field based this theory is as below:

$$\begin{aligned} u(x,y,z) &= -z\frac{\partial w_0(x,y)}{\partial x} + \frac{h}{\pi}\sin\frac{\pi z}{h}\phi(x,y) \\ v(x,y,z) &= -z\frac{\partial w_0(x,y)}{\partial y} + \frac{h}{\pi}\sin\frac{\pi z}{h}\psi(x,y) \\ w(x,y,z) &= w_0(x,y) + \frac{h}{\pi}\cos\frac{\pi z}{h}\xi(x,y) \end{aligned} \tag{70}$$

where ϕ, ψ, ξ and w are the unknown parameter in this theory.

Manuscript received by Editorial Board, August 02, 2014;
final version, March 11, 2015.

REFERENCES

[1] Kirchhoff G.: Über das Gleichgewicht und die Bewegung einer elastischen Scheibe, *J. Reine Angew. Math.*, 1859, (40): 51-88.
[2] Mindlin R.D.: Influence of rotary inertia and shear on flexural motions of isotropic elastic plates, Trans. ASME J. Appl. Mech., 1951, 18, 31-38.
[3] Reissner E.: The effect of transverse shear deformation on the bending of elastic plates, Trans ASME J. Appl. Mech., 1945, 12(2): 69-77.
[4] Reddy J.N.: A simple higher-order theory for laminated composite plates, Trans. ASME J. Appl. Mech., 1984, 51: 745-752.
[5] Reddy J.N., Phan N.D.: Stability and vibration of isotropic, orthotropic and laminated plates according to a higher-order shear deformation theory, J. Sound Vib., 1985, 98(2): 157-170.
[6] Srinivas S., Joga Rao C.V., Rao A.K.: Bending, vibration and buckling of simply supported thick orthotropic rectangular plate and laminates, Int. J. Solids Struct., 1970, 6(11), 1463-1481.
[7] Whitney J.M., Sun C.T.: A higher order theory for extensional motion of laminated composites, Journal of Sound and Vibration, 1973, 30: 85-97.
[8] Hanna N.F., Leissa A.W.: A higher order shear deformation theory for the vibration of thick plates, J. Sound Vib., 1994, 170(4): 545-555.
[9] Bhimaraddi A., Stevens L.K.: A higher order theory for free vibration of orthotropic, homogeneous, and laminated rectangular plates, J. Appl. Mech., 1984, 51: 195-198.
[10] Kant T.: Numerical analysis of thick plates, Comput. Methods Appl. Mech. Eng., 1982, 31(1): 1-18.
[11] Lo K.H., Christensen R.M., Wu E.M.: A high-order theory of plate deformation. Part 1: Homogeneous plates, J. Appl. Mech., 1977, 44(4): 663-668.
[12] Shimpi R.P.: Refined plate theory and its variants, AIAA J., 2002, 40(1): 137-146.
[13] Shimpi R.P., Patel H.G.: A two variable refined plate theory for orthotropic plate analysis, Int. J. Solids Struct., 2006, 43(22): 6783-6799.
[14] Shimpi R.P., Patel H.G.: Free vibrations of plate using two variable refined plate theory, J. Sound Vib., 2006, 296(4-5): 979-999.
[15] Kim S.E., Thai H.T., Lee J.: Buckling analysis of plates using the two variable refined plate theory, Thin Wall. Struct., 2009, 47(4): 455-462.
[16] Kim S.E., Thai H.T., Lee J.: A two variable refined plate theory for laminated composite plates, Compos. Struct., 2009, 89(2): 197-205.

[17] Thai H.T., Kim S.E.: Free vibration of laminated composite plates using two variable refined plate theory, International Journal of Mechanical Sciences, 2010, 52: 626-633.
[18] Thai H.T., Kim S.E.: Levy-type solution for buckling analysis of orthotropic plates based on two variable refined plate theory, Composite Structures, 2011, 93: 1738-1746.
[19] Thai H.T., Kim S.E.: Levy-type solution for free vibration analysis of orthotropic plates based on two variablerefined plate theory, Applied Mathematical Modelling, 2012, 36: 3870-3882.
[20] Narendar S.: Buckling analysis of micro-/nano-scale plates based on two–variable refined plate theory incorporating nonlocal scale effects, Composite Structures, 2011, 93: 3093-3103.
[21] Malekzadeh P., Shojaee M.: A two-variable first-order shear deformation theory coupled with surface and nonlocal effects for free vibration of nanoplates, Composite Structures, 2013, 95: 443-452.
[22] Venstel E., Krauthammer T.: Thin Plates and Shells-Theory, Analysis and Applications, Marcel Dekker Inc., New York, 2001.
[23] Voyiadjis G.Z., Kattan P.I.: Thick rectangular plates on an elastic foundation, J. Eng. Mech., 1986, 112(3): 1218-1240.
[24] Liew K., Han J., Xiao Z., Du H.: Differential quadrature method for Mindlin plates on Winkler foundations, Int. J. Mech. Sci., 1996, 38(4): 405-421.
[25] Hasani A., Saidi A., Ehteshami H.: Accurate solution for free vibration analysis of functionally graded thick rectangular plates resting on elastic foundation, Composite Structures, 2011, 93(7): 1842-1853.
[26] Korhan O., Daloglu A., Karakas A.: A parametric study for thick plates resting on elastic foundation with variable soil depth, Appl. Mech., 2013, 83(4): 549-558.
[27] Ghugal Y.M., Sayyad A.S.: A Static Flexure of Thick Isotropic Plates Using Trigonometric Shear Deformation Theory, Journal of Solid Mechanics, 2010, 2(1): 79-90.
[28] Navier C.L.M.N.: Bulletin des Science de la Societe Philomarhique de Paris, 1823.

Analiza ugięcia grubych płyt spoczywających na podłożu sprężystym z wykorzystaniem udoskonalonej teorii z dwiema zmiennymi

S t r e s z c z e n i e

W publikacji wykorzystano udoskonaloną teorię płyty z dwiema zmiennymi do analizy grubych płyt spoczywających na sprężystym podłożu. Teoria ta, która zawiera tylko dwa nieznane parametry, pozwala przewidzieć paraboliczną zmienność naprężeń ścinających. W teorii jest spełniony warunek zerowej trakcji na powierzchni płyty bez użycia współczynnika korekcyjnego dla ścinania. Stosując zasadę minimum energii potencjalnej wyprowadzono równania rządzące dla płyt prostokątnych o prostym podparciu spoczywających na sprężystym podłożu Winklera. Do rozwiązania otrzymanego układu równań sprzężonych zaadoptowano metodę Naviera. Obecna teoria pozwoliła rozwiązać szereg przykładowych problemów płyt przy różnych warunkach obciążenia. Porównanie otrzymanych rezultatów z uzyskanymi w innych znanych teoriach wykazuje doskonalą efektywność stosowanej teorii w modelowaniu grubych płyt spoczywających na podłożu sprężystym. Przestudiowano także wpływ modułu sprężystości podłoża, grubości płyty i typu obciążenia. Wyniki pokazują, że ugięcia płyty maleją przy wzroście modułu sprężystości podłoża i grubości płyty.